The Pharmacological Mechanisms of Mori Folium and Eucommiae Cortex Extracts against Immunosuppression from Network Pharmacology Perspectives

Jinde Liu , Qiao Rong , Chunxiao Zhang , Ali Tariq , Lin Li , Yongning Wu , Feifei Sun *

Posted Date: 17 October 2023

doi: 10.20944/preprints202310.0991.v1

Keywords: Mori Folium; Eucommiae Cortex; immunosuppression; network pharmacology; molecular docking; molecular dynamics simulations

Article

The Pharmacological Mechanisms of Mori Folium and Eucommiae Cortex Extracts Against Immunosuppression from Network Pharmacology Perspectives

Jinde Liu [1,+], Qiao Rong [1,+], Chunxiao Zhang [1], Ali Tariq [3], Lin Li [1], Yongning Wu [2] and Feifei Sun [1,2,*]

[1] Animal-Derived Food Safety Innovation Team, Anhui Agricultural University, Hefei, 230036, China; 13141212481@163.com

[2] NHC Key Laboratory of Food Safety Risk Assessment, China National Center for Food Safety Risk Assessment, Chinese Academy of Medical Science Research Unit (2019RU014), Beijing 100017, China; sunff@ahau.edu.cn

[3] College of Veterinary Sciences, University of Agriculture Peshawar, Peshawar, Pakistan; tariq.ali.khattak@aup.edu.pk

* Correspondence: Feifei Sun, E-mail: 13141212481@163.com. Address: Changjiang west road No.130, Shushan District, Hefei, P.R.China

+ These authors contributed equally to this work.

Abstract: It's been reported that Mori Folium (MF) and Eucommiae Cortex (EC) exhibit pharmacological effects on the treatment of immunosuppression. However, the mechanism of MF and EC against immunosuppression remains unclear. This study aims to explore the mechanism of action of MF and EC for the treatment of immunosuppression through network pharmacology, molecular docking, molecular dynamics simulations and animal experiments. As a result, 11 critical components, 9 hub targets, and related-signaling pathways of treatment of immunosuppression were obtained based on network pharmacology. The molecular docking suggested that 11 critical components exhibited great binding affinity to 9 hub targets of immunosuppression. The molecular dynamics simulations results showed that (-)-Tabernemontanine-AR, beta-sitosterol-AR and Dehydrodieugenol-HSP90AA1 complexes are stably bound. Additionally, in the animal experiments, the treated group results compared to the control group suggest that MF and EC have a significant effect on the treatment of immunosuppression. Therefore, the MF and EC treatment for immunosuppression may take effects in a multi-component, multi-target, and multi-pathway manner. The results would provide novel insights into the treatment of immunosuppression in humans.

Keywords: Mori Folium; Eucommiae Cortex; immunosuppression; network pharmacology; molecular docking; molecular dynamics simulations

1. Introduction

The immune system plays an important role in anti-infection, anti-tumors as it acts as a body's defense system by protecting our body cells, tissues, and organs from invading infections by harmful microorganisms and other disease-causing microbes [1,2]. Immunomodulation is the interaction between immune cells and immune molecules in the immune system, as well as with other systems such as the neuroendocrine system, to maintain the body at the most appropriate level. It involves two major mechanisms: immune-stimulation and immunosuppression [3], where the immunosuppression refers to the inhibition of the immune response and is becoming increasingly common, especially when patients received transplanted organs or bone marrow [2].

Morus alba L., belonging to the Moraceae family, is one of the most valuable plants and rich in natural products, whose pharmaceutical name is Mori Folium (MF) [4,5]. Mori Folium contains a

 doi:10.20944/preprints202310.0991.v1

variety of active ingredients, such as polysaccharides [6], flavonoids [7], alkaloids [8], etc. The comprehensive effects of these active ingredients reflect the pharmacological effects of MF, including antidiabetic, anti-inflammatory, antibacterial, cardiovascular and cardioprotective, hypolipidemic, antioxidant, and antiatherogenic abilities [9,10].

Eucommiae Cortex (EC) is derived from the dried bark of Eucommia ulmoides Oilv., where active compounds are separated and analyzed by modern chemical methods, and a total of 112 compounds are identified, mainly including lignans, iridoids, phenolics, steroid and terpenoids and flavonoids [11]. Currently, many studies have shown that the pharmacological effects of EC are antihypertensive, hypolipidemic, anti-obesity, antidiabetic, neuroprotective, antioxidative, antifatigue, anti-aging, antitumor, anti-inflammatory and enhancing immune-function [11].

Network pharmacology is a new field combining traditional Chinese medicine (TCM) and network pharmacology, which is based on the theory of system biology and the viewpoint of network pharmacology. Network pharmacology facilitate the under-standing of the compatibility law of prescriptions, identification of TCM medicine, prediction of disease-related targets and the action mechanism of TCM [12]. In this study, the network pharmacology, molecular docking and molecular dynamics simulations methods were used to explore the pharmacological and molecular mechanisms of the anti- immunosuppression activity of Mori Folium and Eucommiae Cortex (MFEC) extracts. And the underlying mechanism of MFEC would provide a new insight into the screening of potential bioactivity and facilitate the development of drugs for anti-immunosuppression treatment from the active compounds.

2. Materials and Methods

2.1. Animal experiments

The animals were housed in the animal house of Anhui Agricultural University, with commercial standard diets and water ad libitum. And among the experimented animals, the half is males and the other half is females. Besides, in current study, all animal experiments completely comply with the ARRIVE guidelines and conducted in accordance with the U.K. Animals (Scientific Procedures) Act, 1986 and associated guidelines, EU Directive 2010/63/EU for animal experiments, or the National Research Council's Guide for the Care and Use of Laboratory Animals.

In this study, fifty mice were randomly divided into five groups, with each group of ten mice: control group, model group, MF group, EC group and MFEC group. After one week accommodation, on the 8th-10th day, except the control group, the other groups were intraperitoneally injected with cyclophosphamide at the rate of 80 mg/kg once a day. The control group was injected with the same amount of normal saline. On the 11th-17th day, MF group, EC group and MFEC group were fed with 200 mg/kg MF, EC, MFEC respectively. The other groups were fed with the same amount of normal saline. All the experiments pertaining to animals comply with the commonly-accepted “3R”, according to the guideline of Anhui Agricultural University about the protection of animals. The spleen of mice was collected and weighted (g), and the spleen index of mice was calculated as follows:

The spleen index (%)=spleen weight (g)/body mass of mice (g) x100%

Additionally, the IF-2, IF-6 and TNF-α level in serum was determined according to the ELISA kits for mouse (Shanghai Jianglai Biotechnology Co., Ltd., Shanghai, China), and 100 μL of negative control, standard or diluted serum sample to be tested were added to the microtiter plate to make duplicate wells. The microtiter plate was covered with film, placed horizontally, and incubated at room temperature for 60 min. After discarding the liquid, wash the plate 4 times with washing solution, dry the plate after each operation. Add 100 μL of enzyme-labeled antibody to each well, add the mem-brane, and incubate at room temperature in the dark for 30 min. Similarly, after dis-carding the liquid, wash it with washing solution for 4 times, and dry the plate after each operation. Add 100 μL of TMB substrate solution to each well, and incubate at room temperature in the dark for 10 min, then add 100 μL of stop solution to each well to stop the reaction. The optical density value (OD value) of each well was measured at the wavelength of 450 nm by microplate reader.

 doi:10.20944/preprints202310.0991.v1

2.2. Database construction of active ingredients and potential targets

Chemical ingredients of MFEC were obtained from Traditional Chinese Medicine Database and Analysis Platform (TCMSP) (https://old.tcmsp-e.com/tcmsp.php). The active compounds were selected according to the pharmacokinetics parameters including absorption, distribution, metabolism, and excretion. Basically, the criteria for the related parameters were set follows: oral bioavailability (OB), not less than 30% and drug-likeness (DL), not less than 0.18.

The potential targets of the active ingredients were obtained from TCMSP, TCM-ID (http://119.3.41.228:8000/tcmid/), PubChem (https://pubchem.ncbi.nlm.nih.gov/) and Swiss Target Prediction database (http://www.swisstargetprediction.ch/). Also, all the targets were integrated and the duplicates were removed.

2.3. Acquisition and screening of immunosuppression-associated targets

GeneCards database (https://www.genecards.org/) was used to extract the immunosuppression-related targets, and the median value of relevance score was used to screen the obtained targets. Only the targets with inference score no less than 9.33 were included. Besides, the Uniprot database (https://www.uniprot.org/) was used to convert the obtained disease-related targets and the potential targets of the active ingredients obtained in section 2.2 into the gene symbol formats. By merging all acquired genes, all targets related to immunosuppression were collected to establish a gene-library of anti-immunosuppression targets. The Venny 2.1 tool (https://bioinfogp.cnb.csic.es/tools/venny/) was used to determine the number of intersection genes between MFEC potential targets and disease-related genes, and to plot a Venn diagram.

2.4. Network construction and topological analysis

The network construction and topological analysis were investigated using String 11.5 database (https://string-db.org/) and Cytoscape 3.8.1 software. Intersection ingredients-targets network was constructed to understand the associations between active ingredients and intersection targets of MFEC. Network generation and visualization were performed using Cytoscape software. In order to construct PPI network, common targets were imported into String 11.5 database to generate a network and the topological analysis was conducted using Cytoscape software, where the degree centrality, closeness centrality, as well as the betweenness centrality were obtained to evaluate the central properties of nodes in the network.

2.5. GO and KEGG pathway enrichment analysis

To further elucidate pharmacological mechanisms of MFEC in immunosuppression treatment, Metascape database (https://metascape.org/), a web-based portal where covers a comprehensive gene list annotation, was used to perform Gene Ontology (GO) enrichment analysis and Kyoto Encyclopedia of Genes and Genomes (KEGG) pathway enrichment analysis. The results were analysed and sorted according to the adjusted P value. Additionally, the target-pathway network was established using Cytoscape software.

2.6. Molecular docking verification

The molecular docking was performed to predict the binding affinity and interactions between the targets with the active ingredients. Based on the topological parameters of the ingredients-targets and PPI networks, ingredients and targets with more than 2-fold the median value of degree were selected as candidate ligands and recep-tors for molecular docking. The software ChemBio3D 19.0 was used to calculate minimizing energy and the ligand structures were exported by MOL 2 format. The 3D structures of selected receptors were screened and downloaded from the RCSB PDB database (https://www.rcsb.org/,). The Sybyl-x 2.1.1 software could perform the molecular docking of active compounds with putative targets. All the softwares and databases used in this study were described in supplementary information **Table S4**.

Preprints (www.preprints.org) | NOT PEER-REVIEWED | Posted: 17 October 2023 doi:10.20944/preprints202310.0991.v1

2.7. Molecular dynamics simulations

The above part of molecular docking results (arachidonic acid-HSP90AA1; Dehydrodieugenol-HSP90AA1; icosa-11,14,17-trienoic acid methyl ester-HSP90AA1; (-)- Tabernemontanine-AR; beta-carotene-AR; beta-sitosterol-AR) were performed by Gromacs 2020.6 software for molecular dynamics simulations. The simulation system was adjusted to a sodium chloride solution at 37°C in order to replicate the actual human in vivo environment. Considering the active ingredient of MF and EC as multi-carbon ring skeleton structures, Charmm36 force field and TIP3P water model was chosen for MDs. During the MDs, the relevant hydrogen bonds are constrained by the Linear Constraint Solver (LINCS) algorithm with the integration step of 2 fs, while the non-bond interaction cut-off value is set to 10 Å and updated every 10 steps. And the electrostatic interactions are calculated using the Particle-mesh Ewald (PME) with a cut-off value of 1.2 nm. In order to optimize the original conformation of the protein in the solvent, the protein receptor-ligand small molecule complex was pre-equilibrated for 100 ps prior to simulations, followed by canonical ensemble (NVT) equilibration for 100 ps using a modified Berendsen temperature coupling algorithm with the coupling time constant of 0.1 ps, which allowed the complex to be warmed up to 310 K with the solvent system. Subsequently, the solvent and complex were pressure equilibrated, while the pressure was increased to 1 bar using a Berendsen constant pressure with constant-pressure and constant-temperature (NPT) equilibration of 100 ps. Finally, MDs of the complex were performed for 50 ns.

3. Results

3.1. Mice spleen index, IL-2, IL-6, and TNF-α level in serum

It can be seen from **Figure 1** that compared with the control group, the spleen index of the mice in the model group decreased. After treatment with MF, EC and MFEC, the spleen index of the mice increased compared with the model group, and the spleen index of the MFEC group increased more obviously, but statistical analysis showed no significant difference. Comparing the levels of TNF-α in all groups, the content of TNF-α in the mf group was slightly lower than that in the control group, but there was no significant change in the other groups. Taken together, these data indicate that the drug may have a certain therapeutic effect on the immunosuppression of mice.

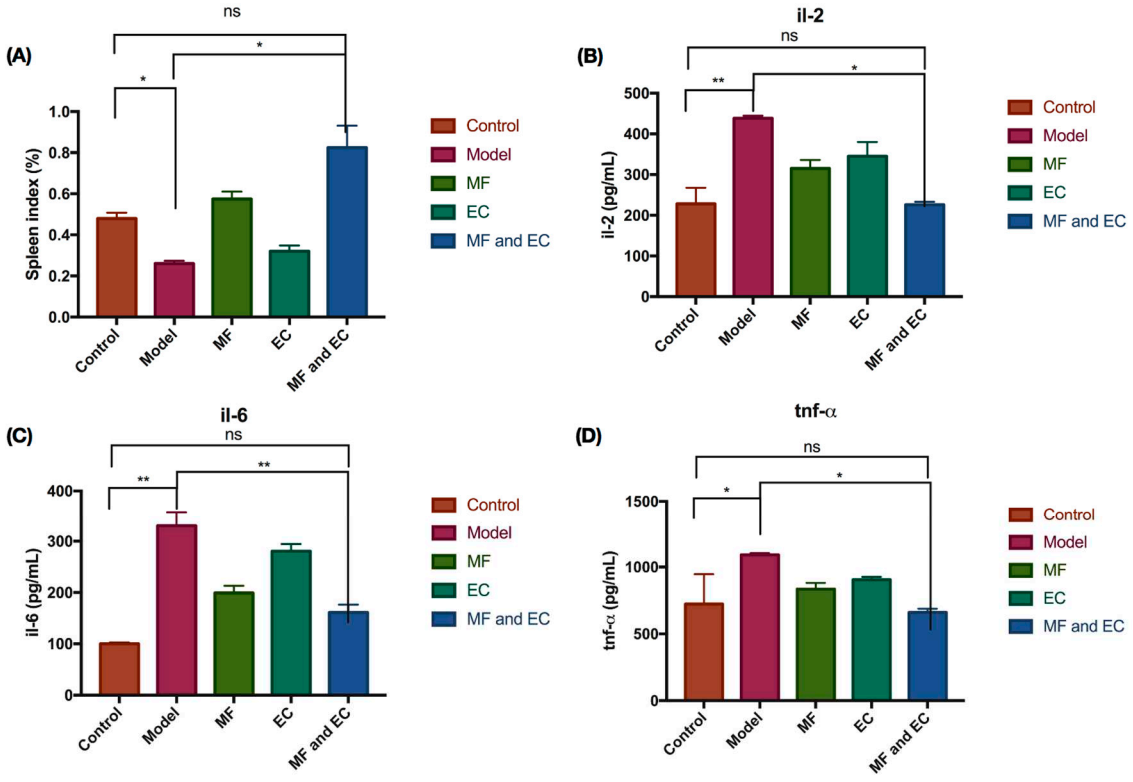

Preprints (www.preprints.org) | NOT PEER-REVIEWED | Posted: 17 October 2023 doi:10.20944/preprints202310.0991.v1

Figure 1. TMF and EC inhibit cyclophosphamide-induced inflammation in mice. (A) The spleen index of mice for control group, inflammation group, and treatment with MF, or EC, or MF and EC. (B, C, D) The expression level of IL-2, IL-6, and TNF-α. Com-pared with control group, the spleen index in the model group decreased whereas the expression level of pro-inflammatory factors IL-2, IL-6, and TNF-α increased in the model group. (*P>0.1, **P>0.01, ***P>0.001, ns stands for no significant difference; t-test and ANOVA analysis).

3.2. Database construction of active ingredients and potential targets

Based on the criteria of the OB≥ 30% and DL≥ 0.18, a total of 53 active ingredients (25 in MF, 24 in EC, 4 common ingredients, in supplementary materials **Table S1**) were retrieved in TCMSP database. All the potential targets of active ingredients were found in TCMSP, TCM-ID, Swiss Target Prediction and Pubchem database. After removing duplicates, 423 potential targets were screened out of the two traditional Chinese medicines.

3.3. Immune suppression-related targets

The immunosuppression-associated targets were retrieved in the GeneCards database. As a result, a total of 11461 disease-related genes were obtained. Based on 3 times screenings of the median value, 1435 disease-related genes were selected. Furthermore, 204 common targets (in supplementary materials **Table S2**) between MFEC targets and disease-related targets were filtered as the critical targets for further study (**Figure 2A**).

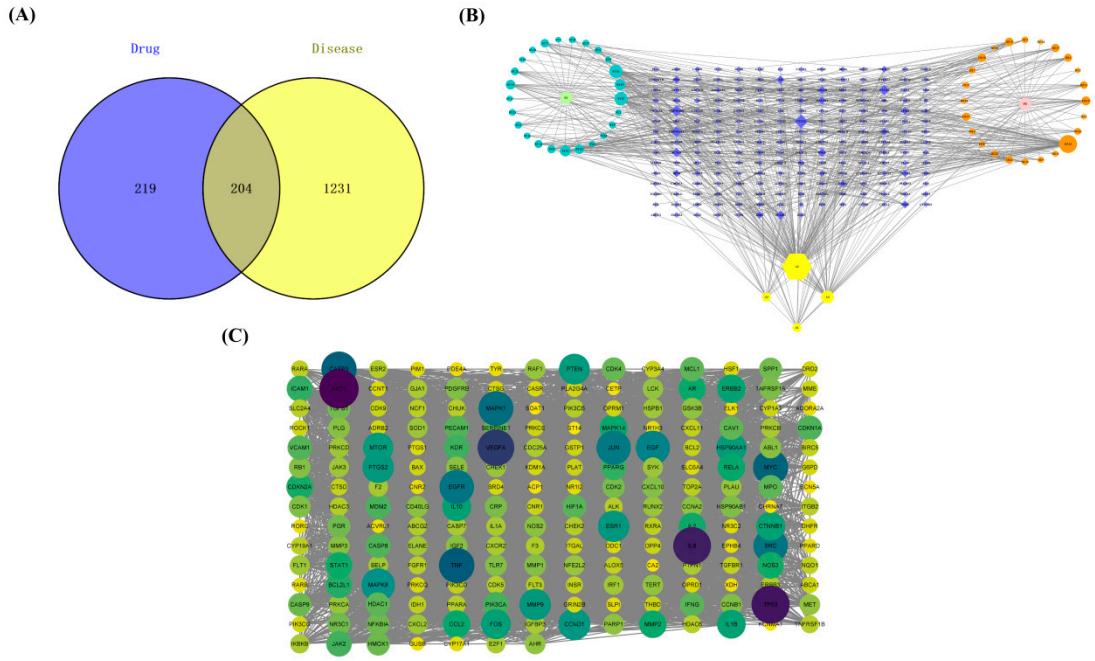

Figure 2. Construction of database and network. (A) Venny diagram of MFEC targets and immune suppression disease gene set. (B) Network of ingredient-target interaction: Lake blue dots represent MF compounds, light green origin represents drug MF, orange dots are EC compounds, pink dots are EC drugs, yellow hexagonal nodes are the common compounds of MFEC, and blue diamonds are the intersection targets of drugs and diseases. (C) PPI network.

3.4. Intersection compound-targets network

The compound-target interaction network was visualized in **Figure 2B** with 259 nodes and 665 edges by Cytoscape. In the network, nodes represent the screened drug, active ingredients and genes, while the connections between the nodes represent the interactions between these biological analyses. In the current study, active compounds with degree 2-fold higher than the median value were

Preprints (www.preprints.org) | NOT PEER-REVIEWED | Posted: 17 October 2023 doi:10.20944/preprints202310.0991.v1

selected to perform molecular docking. These 11 active compounds were shown in supplementary materials **Table S3**.

3.5. PPI network

To analyze the protein-protein interaction, the 204 common targets of ingredients and diseases were imported into the String database and Cytoscape to show complex interaction between proteins encoded by these targets. The PPI network covered 203 nodes (the protein IGHG1 was not identified) and 4897 edges (**Figure 2C**). Among the 203 proteins, AKT1, AR, CASP3, HSP90AA1, JUN, MAPK14, MMP2, PTSG2, TNF, were hub proteins finally selected as putative targets to conduct molecular docking.

3.6. GO and KEGG enrichment analysis

3.6.1. GO enrichment

GO enrichment analysis was performed using Metascape software on 204 common targets of immunosuppression and Mori Folium and Eucommiae Cortex in terms of biological process (BP), cellular composition (CC) and molecular function (MF)[13]. As seen in **Figure 3A**, Biological process mainly included positive regulation of vitamin D biosynthetic process, positive regulation of calcidiol 1-monooxygenase activity, response to carbon monoxide, activation of cysteine-type endopeptidase activity involved in apoptotic signaling pathway and positive regulation of apoptotic process involved in morphogenesis. The cellular composition mainly enriched in Bcl-2 family protein complex, cyclin/CDK positive transcription elongation factor complex and nuclear cyclin-dependent protein kinase holoenzyme complex. The molecular function mainly involved phosphatidylinositol-3,4-bisphosphate 5-kinase activity, BH3 domain binding, ErbB-3 class receptor binding, 1-phosphatidylinositol-4-phosphate 3-kinase activity, phosphatidylinositol-4,5-bisphosphate 3-kinase activity.

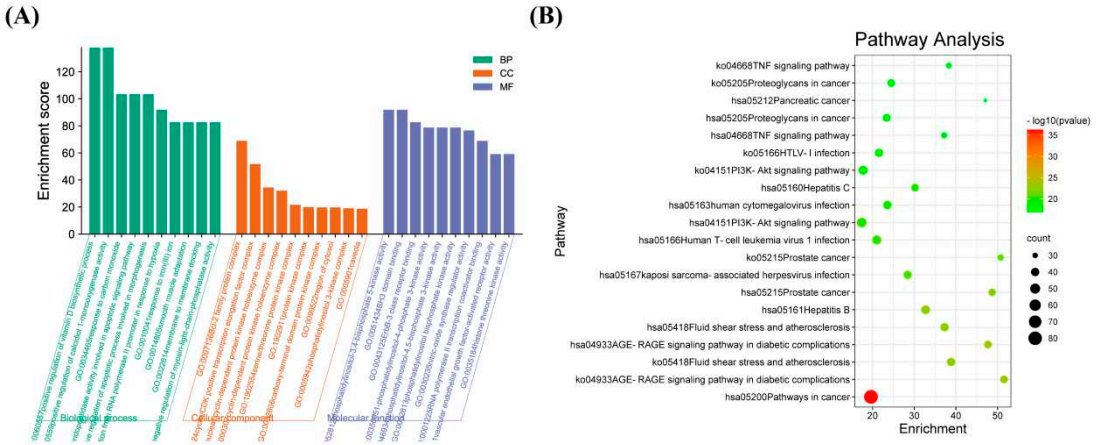

Figure 3. GO and KEGG enrichment analysis. (A) GO enrichment. The green bars represent the analysis of BP, the orange ones represent the analysis of CC, and the blue ones represent the analysis of MF; (B) Bubble diagram of KEGG pathways. The horizontal axis represents the gene enrichment, while the longitudinal axis represents pathway terms. The bubble's color represents the significance level (p-value) of corresponding pathways: the significance level decreases (p-value increases) from red to green. And the bubble's size represents the gene count of the pathway.

3.6.2. KEGG enrichment

KEGG pathway analysis could indicate possible signal pathway of 204 proteins, and there were 362 pathways been obtained totally. **Figure 3B** and supplementary material **Table S5** showed specific information about the underlying mechanisms involved in MFEC to treat immune suppression. The

Preprints (www.preprints.org) | NOT PEER-REVIEWED | Posted: 17 October 2023 doi:10.20944/preprints202310.0991.v1

top three enriched KEGG pathways were: pathways in cancer, AGE-RAGE signaling pathway in diabetic complications, fluid shear stress and atherosclerosis.

3.7. Molecular docking

9 proteins were selected according to the PPI network and the structure of these nine proteins were downloaded from the PDB database. Sybyl-X software was used to remove water and excess ligands in these 9 proteins and then hydrogenated. The last step in pre-processing the protein was to generate binding pockets. These 9 proteins were docked with 11 active components (obtained in 3.4), the related results were shown in **Table 1**, **Figure 4A**,**B**. In **Table 1**, we could see that among all 11 active compounds, iristectorigenin A, quercetin, acid methyl ester, arachidonic acid might be an important active compound. Among all 9 protein targets, iristectorigenin A had better docking results with AKT1 and AR, and there were three docking sites with each target. Quercetin and CASP3 docking have five binding sites, which is the most in all dockaing. Acid methyl ester binds to HSPAA1 and TNF in a docking site, respectively. Arachidonic acid has the best docking effect with four of the screened targets and has a high score. In addition to two binding sites with PTGS2, arachidonic acid has one docking site with JUN, MAPK14 and MMP2.

Table 1. Molecular docking results.

Protein	Compound	Binding site	Total score
AKT1	Iristectorigenin A	A/SER56, A/LEU110, A/GLN59	5.0365
AR	Iristectorigenin A	A/ASN705, A/GLN711, A/MET745	6.5950
CASP3	quercetin	A/ARG64, A/SER205, A/GLY165, A/ARG164, A/GLU123	6.2159
HSP90AA1	acid methyl ester	A/GLN23	11.3399
JUN	arachidonic acid	B/MET253	4.3453
MAPK14	arachidonic acid	A/HIS148	10.0545
MMP2	arachidonic acid	A/ASN573	7.0050
PTGS2	arachidonic acid	B/GLU486, B/ARG438	6.0676
TNF	acid methyl ester	D/TYR151	7.4725

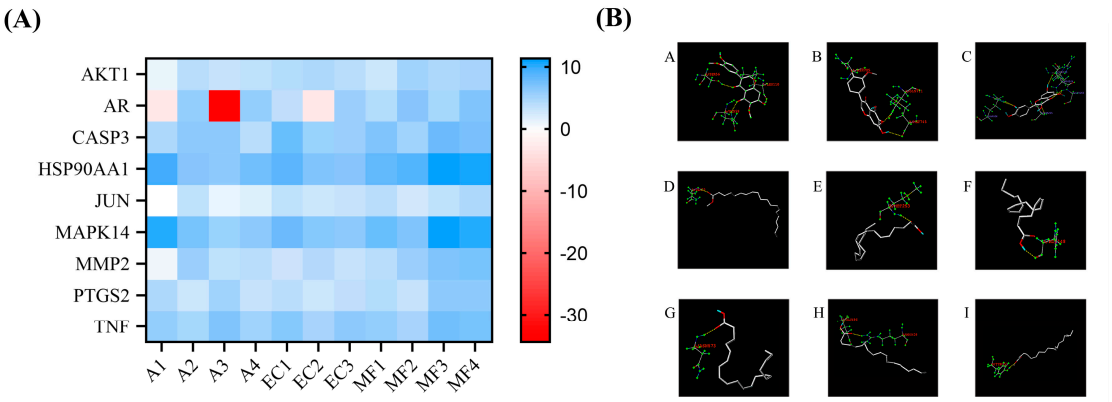

Figure 4. Molecular docking. (A) Heat map of total score between compounds and proteins. (B) the binding site of molecular docking: docking results of AKT1 (A) and AR (B) with iristectorigenin A; docking results of CASP3 (C) and quercetin; docking results of HSP90AA1(D) and TNF(I) with acid methyl ester; docking results of JUN (E), MAPK14 (F), MMP2 (G) and PTGS2 (H) with arachidonic acid.

3.8. Molecular dynamics simulations

To further validate the binding stability of drug active ingredients with AR and HSP90AA1 in vivo, the analysis of Root Mean Square Deviation (RMSD), Root Mean Square Fluctuation(RMSF), Radius of Gyration (Rg) and Hydrogen bond (Hbond) were obtained by Gromacs 2020.6 software.

Preprints (www.preprints.org) | NOT PEER-REVIEWED | Posted: 17 October 2023 doi:10.20944/preprints202310.0991.v1

RMSD was used to analyze the binding stability of the AR and HSP90AA1 to the corresponding ligand receptor in the MDs. **Figure 5A** showed that the (-)-Tabernemontanine-AR complex reached dynamic equilibrium within a short time (10 ns) and the RMSD value remained around 0.12 nm until the end of the simulation, indicating that AR bound well with (-)-Tabernemontanine and can form a stable complex. Meanwhile, the binding of AR with beta-sitosterol and beta-carotene reached the equilibrium at 10-15 ns, and its RMSD fluctuation value was less than 0.3 nm, which suggested that was stable drug-protein complex binding. **Figure 5B** suggested that arachidonic acid-HSP90AA1 and icosa-11,14,17-trienoic acid methyl este-HSP90AA1 always had large fluctuations in the RSMD curves during the MDs, indicating that the active ingredient of the drug could not bind stably to the protein target. RMSF was used to reflect the fluctuations and the degree of motion drasticity of protein residues throughout the MDs. **Figure 5C**,**D** showed that AR and HSP90AA1 residues had greater flexibility and adaptability when key drug active ingredients were bound to hub protein target.

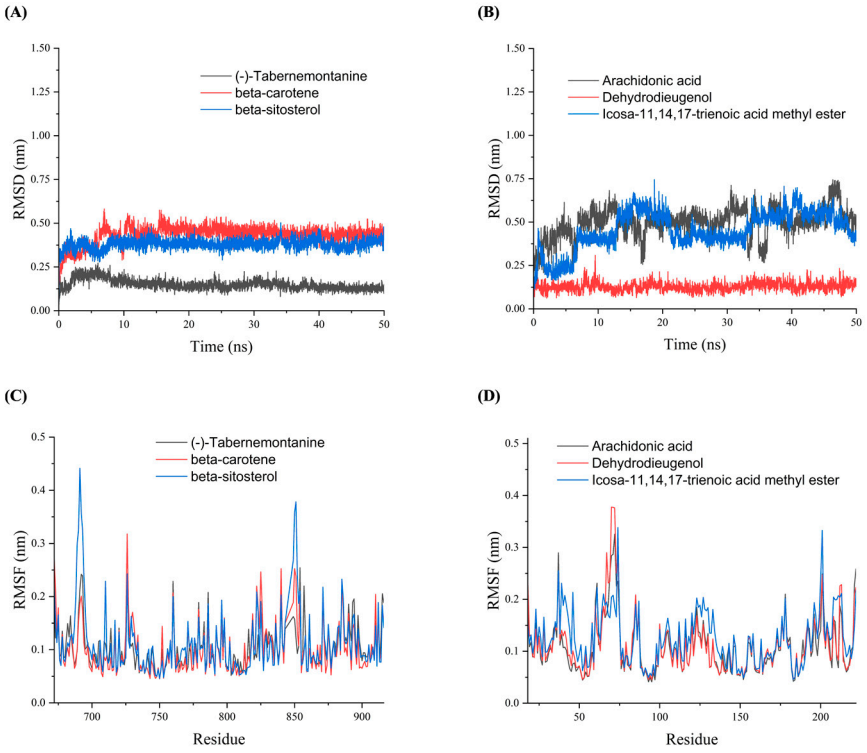

Figure 5. The RMSD and RMSF plots of molecular dynamics simulation. (A) RMSD plots of AR with (-)- Tabernemontanine, beta-carotene and beta-sitosterol. (B) RMSF plots of HSP90AA1 with arachidonic acid, Dehydrodieugenol, icosa-11,14,17-trienoic acid methyl ester.

Rg indicated the tightness of the overall structure of the protein [14], as well as characterized the changes in peptide chain relaxation of the protein during the simulation. **Figure 6A** indicated that the complexes formed by AR bounds to corresponding three drug active molecules had more stable radius of gyration and they gradually decreased in the MDs, which suggested that the proteins gradually converge and the complex structures become stable after binding to the small molecules. The Rg curves of HSP90AA1 showed some fluctuations (**Figure 6B**). As was seen in **Figure 6C**, beta-sitosterol-AR complex formed hydrogen bonds only in part of the time period, and (-)-Tabernemontanine-AR complex basically remained more than 1 hydrogen bonds during the simulation. The interaction between beta-carotene with AR never formed hydrogen bond **(Figure 6C)** because beta-carotene-AR complex structure haven't hydrogen bond and the interaction be dominated by hydrophobic interactions. **Figure 6D** showed that the number of hydrogen bonds of arachidonic acid-HSP90AA1 complex were low throughout the MDs. **Figure 6D** showed that the number of hydrogen bonds formed by the icosa-11,14,17-trienoic acid methyl ester-HSP90AA1 complex had 1-2 hydrogen bonds. Dehydrodieugenol-HSP90AA1 complex maintained one hydrogen

Preprints (www.preprints.org) | NOT PEER-REVIEWED | Posted: 17 October 2023 doi:10.20944/preprints202310.0991.v1

bond for most of the time throughout the MDs, which indicates that Dehydrodieugenol is more stable in binding to HSP90AA1 combined with RMSD analysis.

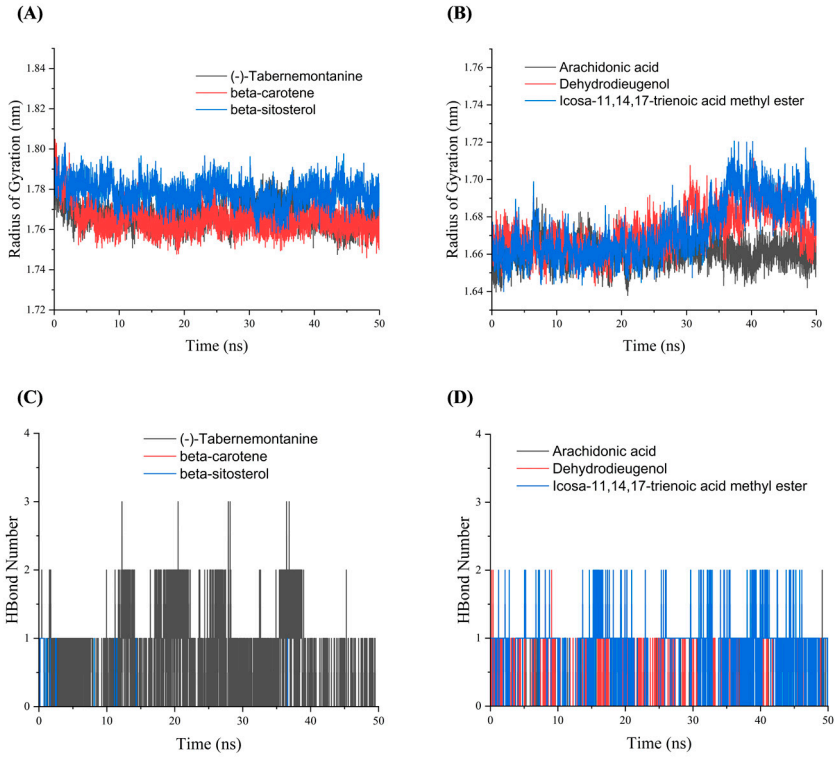

Figure 6. The Rg and Hbond plots of molecular dynamics simulation. (A) Rg plots of AR with (-)-Tabernemontanine, beta-carotene and beta-sitosterol. (B) Hbond plots of HSP90AA1 with arachidonic acid, Dehydrodieugenol, icosa-11,14,17-trienoic acid methyl ester.

4. Discussion

In recent decades, TCM has attracted worldwide attention due to its exact curative effects, relatively less low toxicity and low cost. Due to the complexity components of TCM and the various biological systems where they were involved, how to elucidate the mechanism of action has become a challenge [12,15]. Network pharmacology takes the main active ingredients and target proteins of TCM as nodes, and edges to represent their interactions by generating an interaction network, to elucidate the mechanism of action of TCM prescriptions from the molecular level [16].

In the present study, the network pharmacology is used to explore the possibility of MFEC in the treatment of immunosuppression. The obtained relevant targets were used to dig out the putative related pathways, and to speculate the possible mechanism of MFEC treatment of immunosuppression. Also, molecular docking was used to verify the key components and targets of MFEC involved in the treatment of immunosuppression.

During the active component data-mining of MFEC, a total of 53 active components were collected. Finally, 11 critical components were selected according to the PPI and topological parameters. The 11 components were icosa-11,14,17-trienoic acid methyl ester, iristectorigenin A, arachidonic acid, tetramethoxyluteolin in MF; dehydrodieugenol, (-)-tabernemontanine, (9R)-6'-methoxycinchonan-9-ol in EC, and their common active ingredients quercetin, kaempferol, beta-sitosterol, beta-carotene. These 11 compounds mainly belong to flavonoids, alkaloids, phenolics, terpenes, phytosterols and organic acids that play pharmacological effects in MFEC. Both flavonoids and phenolic active ingredients in MFEC belong to polyphenolic compounds and they contain a large number of aromatic hydroxyl groups, which account for their anti-inflammatory, anti-glycemic pharmacological effects, and prevent oxidative dam-age and cell death [11,17,18]. In addition, studies have shown that kaempferol can alleviate neuronal damage caused by kainic acid-induced epilepsy in mice, restore the proliferation of T lymphocytes to a certain extent, reduce the phagocytic function

 doi:10.20944/preprints202310.0991.v1

of macrophages, and inhibit the apoptosis of thymocytes [19]. Besides, kaempferol has certain immunomodulatory effects [19]. To explore the protective effect of organic ac-ids on inflammatory injury in acute tracheobronchitis, LPS wad used to establish respiratory inflammation in mice [20]. Results showed that organic acids could treat acute tracheobronchitis by regulating the TLR4/NF-κB signaling pathway, indicating that organic acids have certain anti-inflammatory effects.

The pharmacological effects of alkaloids are very extensive, and can be used for anticancer, antimalarial, antiviral, antihypertensive, antispasmodic, antiarrhythmic, analgesic, antibacterial and antidiabetic, as well as central nervous system stimulants, muscle relaxants, with vasodilatory properties [21]. The beta-sterols in MFEC belong to the class of phytosterols that have been shown to have cholesterol-lowering, anti-cancer, anti-atherosclerotic, anti-inflammatory and antioxidant effects [22]. Be-ta-carotene belongs to the group of carotenoids in terpenoids and has been proven to be the most abundant pigment and fat-soluble antioxidant in nature [23]. In addition, studies have demonstrated that the addition of fully oxidized beta-carotene to the feed can enhance the immunity and performance of sows [24].

Comprehensive analysis of GO enrichment results showed that the active com-ponents in MFEC may act on organisms through nucleus, cytoplasm, membrane, cyto-sol and organelle membrane, exert the molecular functions of phosphatidylinosi-tol-3-kinase (PI3K) family protein kinases, BH3 domain binding, nitric oxide and other synthase regulators, vascular endothelial growth factor (VEGF) activator receptors, RNA polymerase 2 transcription coactivator, and so on, participate in the reaction to carbon monoxide and iron ions, positively regulate vitamin D biosynthesis, monooxygenase activity and cell apoptosis in vivo, negative regulation of myosin light chain phosphatase and other series of biological processes, so as to achieve the goal of therapeutic immunosuppression. KEGG enrichment analysis showed that the main signaling pathways involved in the common targets of MFEC and immunosuppression included pathway in cancer, advanced glycation end products and their receptors (AG-Es-RAGE) signaling pathway in diabetic complications, PI3K-Akt signaling pathway, tumor necrosis factor (TNF) signaling pathway, fluid shear stress and atherosclerosis, kapos sarcoma-associated herpes virus infection, hepatitis B and C, prostate and pancreatic cancer. AGEs are heterogeneous glycation products of proteins, lipids and nucleotides, and their receptors are called RAGE, which are multiligand transmembrane receptors of the immunoglobulin superfamily [25]. When the body's redox homeostasis is disrupted, ROS accumulate, resulting in oxidative stress. Studies have shown that some active components in TCM could improve the level of intracellular oxidative stress, reduce the content of AGEs and ROS, and down-regulate the level of oxidative stress by inhibiting the AGEs-RAGE signaling pathway [26]. From the CC analysis, PI3K is a cytoplasmic lipid kinase, which is a heterodimer composed of a regulatory subunit p85 and a catalytic subunit p110. And the active PI3K phosphorylates to generate the second messenger phosphatidylinositol 3,4,5-triphosphate (PIP3), which further induces the phosphorylation of AKt, and thus participates in the regulation of various life processes such as growth, apoptosis, and oxidative stress [27]. TNF is one of the most well-studied cytokines in the immune system, which can regulate various processes such as cell communication, differentiation and death. These regulatory functions are related to various diseases of the body, including the body's autoimmunity [28].

The nine protein targets selected for molecular docking in this study were jointly selected by combining the analysis results of compounds-targets network and PPI network. AKT1, one of the AKT isoforms, is an oncogene that is ubiquitous in neurons as an important downstream substrate in PI3K-Akt signaling pathway [29]. AKT1 also plays a key role in the normal development of the nervous system and memory formation when participating in the regulation of cell survival and growth [30]. When AKT1 is mutated, it can increase the risk of schizophrenia [31]. The androgen receptor (AR) is a ligand-activated nuclear receptor that interacts with the estrogen receptor (ER), glucocorticoid receptor (GR), progesterone receptor (PR) and mineralocorticoid receptor (MR), both belong to the type I nuclear receptor subfamily [32]. AR coordinates the expression of androgen-regulated transcriptomes in the nucleus and is critical for prostate development, homeostasis, and carcinogenesis. Studies have shown that AR outside the nucleus can form a complex with Akt under

 doi:10.20944/preprints202310.0991.v1

androgen stimulation, and induce the phosphorylation and activation of Akt [32,33]. CASP3 is one of the final effector proteins in the apoptotic response. Tian et al. [34]have shown that under hypoxia and nutrient deprivation conditions, the activity of CASP3 in human nucleus pulposus-derived mesenchymal hepatocytes can be enhanced to promote cell apoptosis. HSP90AA1 is the α isoform of the heat shock protein (HSP) family with a molecular weight of 90 kDa. HSP90 has the function of maintaining protein stability and is involved in the arrangement and maintenance of almost the entire cytoskeleton [35]. Additionally, HSP90AA1 can promote autophagy through the PI3K/Akt/mTOR signaling pathway, and inhibit apoptosis through the JNK/P38 signaling pathway to im-prove the drug resistance of osteosarcoma cells [17]. JUN is an important component of the transcriptional activation protein complex AP1 (Activation Protein-1, AP1), which is widely involved in many biological processes such as cell proliferation, differentiation and apoptosis. JUN can form dimers by combining with other components of the AP1 complex to jointly regulate the expression of downstream target genes [36]. MAPK14 belongs to the mitogen-activated protein kinase (MAPK) family of proteins, enhancing the formation of tumor platelet aggregates that interact with lung endothelium to form lung metastases [37]. MMP2 belongs to the family of matrix metalloproteinases (MMPs), which are known as inflammatory mediators [38]. In the process of atherosclerosis (AS), MMP2 can degrade a variety of collagen and basement mem-brane components, lyse the collagen fibers of AS plaques, and reduce the thickness of the fibrous cap at the plaque. high important evaluation factor [39]. PTGS2, also known as cyclooxygenase 2 (COX-2), is a pro-inflammatory factor that is normally not expressed in most tissues. Its expression is induced by a variety of stimuli, such as epi-dermal growth factor (EGF), interleukin-1 (IL-1), and TNF, and inflammatory responses may also induce the production of PTGS2 [40,41]. TNF mainly refers to TNF-α, as the first inflammatory factor in the inflammatory response, TNF can activate lymphocytes and neutrophils, and play a crucial role in initiating and expanding the inflammatory cascade [42].

Molecular docking revealed drug-target and protein-target interactions from the molecular perspective, and MDs have been widely used to study the binding stability between proteins and molecules and evaluate the structural features of protein-ligand systems [43]. Therefore, in this study, we adopted a combination of molecular docking and molecular dynamics simulation to screen the key targets of ML and EC for enhancing immune function and to verify the stability of active ingredient binding to protein targets. The molecular docking results suggests that iristectorigenin A, quercetin, acid methyl ester, arachidonic acid exhibited great binding affinity to 9 hub targets of immunosuppression. From the analysis of the results of RMSD, RMSF, RG and Hbond of MDs, it is clear that (-)-Tabernemontanine-AR, beta-sitosterol-AR and Dehydrodieugenol-HSP90AA1 complexes bind stably. Molecular docking and further MDs validation finally identified AR, MAPK14, TNF and HSP90AA1 as the core targets for immunosuppression.

5. Conclusions

Mori Folium and Eucommiae Cortex extracts have been demonstrated to be effective for the treatment of immunosuppression. However, the underlying mechanism is unclear. In the current study, network pharmacology, molecular docking, molecular dynamics simulations and experiment validation were conducted to decipher the pharmacological mechanisms of MFEC extracts. Our results showed that the interactions were in consistent with the published literatures and could be employed to the treatment for immunosuppression. Generally, network pharmacology analysis is applied to investigate the pharmacological mechanism of TCM. We reckon that it is a good alternative to explore mechanism by combing network pharmacology analysis, molecular docking and molecular dynamics simulation multiple pathways work together to enhance the body's immune function and improve immune suppression. This study provides a theoretical basis for in-depth exploration of the pharmacological effects of MFEC and its mechanism of action in the treatment of immunosuppression.

Supplementary Materials: The following supporting information can be downloaded at the website of this paper posted on Preprints.org. Table S1: Detailed information on active compounds; Table S2:204 common targets (Table S3) between MFEC targets and disease-related targets; Table S3: The information of active

 doi:10.20944/preprints202310.0991.v1

ingredients including 2D structure; Table S4: The softwares and databases used in this study; Table S5: KEGG pathway analysis of MFEC to treat immune suppression.

Author Contributions: Conceptualization, Jinde Liu and Qiao Rong; methodology, Jinde Liu and Chunxiao Zhang; software, Qiao Rong; formal analysis, Chunxiao Zhang; writing – original draft preparation, Jinde Liu and Qiao Rong; writing – review & editing, Ali Tariq; supervision, Yongning Wu and Lin Li; project administration, Feifei Sun; funding acquisition, Feifei Sun.

Funding: This work was funded by Foundation of the higher education institutions of Anhui Province (No. KJ2021A0147), Natural Science Foundation of Anhui Agricultural University (No. 2019zd17), and the Animal-Derived Food Safety Innovation Team (ANRC2021040).

Institutional Review Board Statement: The animal experiments were approved by the Animal Welfare and Ethics Committee of Anhui Agricultural University (protocol code AHAUXMSQ2023052).

Informed Consent Statement: Not applicable.

Data Availability Statement: All data are contained within the manuscript or in Supplemental Materials.

Conflicts of Interest: The authors declare no conflict of interest.

References

1. Li, W. J.; Li, L.; Zhen, W. Y.; Wang, L. F.; Pan, M.; Lv, J. Q.; Wang, F.; Yao, Y. F.; Nie, S. P.; Xie, M. Y. Ganoderma atrum polysaccharide ameliorates ROS generation and apoptosis in spleen and thymus of immunosuppressed mice. *Food Chem Toxicol* **2017,** 99, 199-208.
2. Nicholson, L. B. The immune system. *Essays Biochem* **2016,** 60, 275-301.
3. Raj, S.; Gothandam, K. M. Immunomodulatory activity of methanolic extract of Amorphophallus commutatus var. wayanadensis under normal and cyclophosphamide induced immunosuppressive conditions in mice models. *Food Chem Toxicol* **2015,** 81, 151-159.
4. Li, Y.; Zhang, X.; Liang, C.; Hu, J.; Yu, Z. Safety evaluation of mulberry leaf extract: Acute, subacute toxicity and genotoxicity studies. *Regul Toxicol Pharmacol* **2018,** 95, 220-226.
5. Gryn-Rynko, A.; Bazylak, G.; Olszewska-Slonina, D. New potential phytotherapeutics obtained from white mulberry (Morus alba L.) leaves. *Biomed Pharmacother* **2016,** 84, 628-636.
6. Zhang, Y.; Ren, C.; Lu, G.; Mu, Z.; Cui, W.; Gao, H.; Wang, Y. Anti-diabetic effect of mulberry leaf polysaccharide by inhibiting pancreatic islet cell apoptosis and ameliorating insulin secretory capacity in diabetic rats. *Int Immunopharmacol* **2014,** 22, 248-57.
7. JIANG, Z.-j.; XU, S.-q.; Xing, Y.; HU, X.-m.; PAN, H.-y. Effects of flavonoids in Morus indica on blood lipids and glucose in hyperlipidemia-diabetic rats. *Journal of Chinese Herbal Medicines* **2012,** 4, 314-318.
8. Hu, X. Q.; Thakur, K.; Chen, G. H.; Hu, F.; Zhang, J. G.; Zhang, H. B.; Wei, Z. J. Metabolic effect of 1-Deoxynojirimycin from Mulberry Leaves on db/db Diabetic mice using liquid chromatography-mass spectrometry based metabolomics. *J Agric Food Chem* **2017,** 65, 4658-4667.
9. Ji, T.; Li, J.; Su, S. L.; Zhu, Z. H.; Guo, S.; Qian, D. W.; Duan, J. A. Identification and determination of the polyhydroxylated alkaloids compounds with alpha-Glucosidase inhibitor activity in Mulberry Leaves of different origins. *Molecules* **2016,** 21, 206.
10. Shipra, J.; Srivastava, A. Antibacterial, antifungal and pesticidal activity of plant Morus alba-a novel approach in post harvest technology. *IJASR* **2013,** 3, 157-161.
11. He, X.; Wang, J.; Li, M.; Hao, D.; Yang, Y.; Zhang, C.; He, R.; Tao, R. Eucommia ulmoides Oliv.: ethnopharmacology, phytochemistry and pharmacology of an important traditional Chinese medicine. *J Ethnopharmacol* **2014,** 151, 78-92.
12. Li, S. Exploring traditional chinese medicine by a novel therapeutic concept of network target. *Chin J Integr Med* **2016,** 22, 647-652.
13. Sun, F.; Liu, J.; Tariq, A.; Wang, Z.; Wu, Y.; Li, L. Unraveling the mechanism of action of cepharanthine for the treatment of novel coronavirus pneumonia (COVID-19) from the perspectives of systematic pharmacology. *Arab J Chem* **2023,** 16, 104722.
14. Jiao, Y.; Shi, C.; Sun, Y. Unraveling the role of Scutellaria baicalensis for the treatment of Breast Cancer using network pharmacology, molecular docking, and molecular dynamics simulation. *Int J Mol Sci* **2023,** 24, 3594.

15. Sham, T. T.; Chan, C. O.; Wang, Y. H.; Yang, J. M.; Mok, D. K.; Chan, S. W. A review on the traditional Chinese medicinal herbs and formulae with hypolipidemic effect. *Biomed Res Int* **2014,** 2014, 925302.
16. Luo, T. T.; Lu, Y.; Yan, S. K.; Xiao, X.; Rong, X. L.; Guo, J. Network pharmacology in research of Chinese medicine formula: methodology, application and prospective. *Chin J Integr Med* **2020,** 26, 72-80.
17. Xiao, X.; Wang, W.; Li, Y.; Yang, D.; Li, X.; Shen, C.; Liu, Y.; Ke, X.; Guo, S.; Guo, Z. HSP90AA1-mediated autophagy promotes drug resistance in osteosarcoma. *J Exp Clin Cancer Res* **2018,** 37, 201.
18. Abdelmoaty, M. A.; Ibrahim, M. A.; Ahmed, N. S.; Abdelaziz, M. A. Confirmatory studies on the antioxidant and antidiabetic effect of quercetin in rats. *Indian J Clin Biochem* **2010,** 25, 188-92.
19. 19. Mu, J. J. The regulation of kaemperol on immunological function in vitro and epilepsy of mouse. Master, Jinan University, Guangzhou, 2010.
20. Yang, N.; Li, C.; Tian, G.; Zhu, M.; Bu, W.; Chen, J.; Hou, X.; Di, L.; Jia, X.; Dong, Z.; Feng, L. Organic acid component from Taraxacum mongolicum Hand.-Mazz alleviates inflammatory injury in lipopolysaccharide-induced acute tracheobronchitis of ICR mice through TLR4/NF-kappaB signaling pathway. *Int Immunopharmacol* **2016,** 34, 92-100.
21. Ti, H.; Zhuang, Z.; Yu, Q.; Wang, S. Progress of plant medicine derived extracts and alkaloids on modulating viral infections and inflammation. *Drug Des Devel Ther* **2021,** 15, 1385-1408.
22. Mingrou, L.; Guo, S.; Ho, C. T.; Bai, N. Review on chemical compositions and biological activities of peanut (Arachis hypogeae L.). *J Food Biochem* **2022,** 46, e14119.
23. Saini, R. K.; Nile, S. H.; Park, S. W. Carotenoids from fruits and vegetables: Chemistry, analysis, occurrence, bioavailability and biological activities. *Food Res Int* **2015,** 76, 735-750.
24. Chen, J.; Chen, J.; Zhang, Y.; Lv, Y.; Qiao, H.; Tian, M.; Cheng, L.; Chen, F.; Zhang, S.; Guan, W. Effects of maternal supplementation with fully oxidised β-carotene on the reproductive performance and immune response of sows, as well as the growth performance of nursing piglets. *Br J Nutr* **2021,** 125, 62-70.
25. Soman, S.; Raju, R.; Sandhya, V. K.; Advani, J.; Khan, A. A.; Harsha, H. C.; Prasad, T. S.; Sudhakaran, P. R.; Pandey, A.; Adishesha, P. K. A multicellular signal transduction network of AGE/RAGE signaling. *J Cell Commun Signal* **2013,** 7, 19-23.
26. Al-Hussaini, H.; Kilarkaje, N. Trans-resveratrol mitigates type 1 diabetes-induced oxidative DNA damage and accumulation of advanced glycation end products in glomeruli and tubules of rat kidneys. *Toxicol Appl Pharmacol* **2018,** 339, 97-109.
27. Zughaibi, T. A.; Suhail, M.; Tarique, M.; Tabrez, S. Targeting PI3K/Akt/mTOR pathway by different flavonoids: A cancer chemopreventive approach. *Int J Mol Sci* **2021,** 22, 12455.
28. Brenner, D.; Blaser, H.; Mak, T. W. Regulation of tumour necrosis factor signalling: live or let die. *Nat Rev Immunol* **2015,** 15, 362-374.
29. Tang, F.; Wang, Y.; Hemmings, B. A.; Ruegg, C.; Xue, G. PKB/Akt-dependent regulation of inflammation in cancer. *Semin Cancer Biol* **2018,** 48, 62-69.
30. Dummler, B.; Hemmings, B. A. Physiological roles of PKB/Akt isoforms in development and disease. *Biochem Soc Trans* **2007,** 35, 231-235.
31. Matsuda, S.; Ikeda, Y.; Murakami, M.; Nakagawa, Y.; Tsuji, A.; Kitagishi, Y. Roles of PI3K/AKT/GSK3 pathway involved in psychiatric illnesses. *Diseases* **2019,** 7, 22.
32. Tan, M. H.; Li, J.; Xu, H. E.; Melcher, K.; Yong, E. L. Androgen receptor: structure, role in prostate cancer and drug discovery. *Acta Pharmacol Sin* **2015,** 36, 3-23.
33. Deng, Q.; Zhang, Z.; Wu, Y.; Yu, W. Y.; Zhang, J.; Jiang, Z. M.; Zhang, Y.; Liang, H.; Gui, Y. T. Non-genomic action of androgens is mediated by rapid phosphorylation and regulation of androgen receptor trafficking. *Cell Physiol Biochem* **2017,** 43, 223-236.
34. Tian, D.; Liu, J.; Chen, L.; Zhu, B.; Jing, J. The protective effects of PI3K/Akt pathway on human nucleus pulposus mesenchymal stem cells against hypoxia and nutrition deficiency. *J Orthop Surg Res* **2020,** 15, 29.
35. Hangzo, H.; Banerjee, B.; Saha, S.; Saha, N. Ammonia stress under high environmental ammonia induces Hsp70 and Hsp90 in the mud eel, Monopterus cuchia. *Fish Physiol Biochem* **2017,** 43, 77-88.
36. Meng, Q.; Xia, Y. c-Jun, at the crossroad of the signaling network. *Protein & Cell* **2011,** 2, 889-898.
37. Matsuo, Y.; Amano, S.; Furuya, M.; Namiki, K.; Sakurai, K.; Nishiyama, M.; Sudo, T.; Tatsumi, K.; Kuriyama, T.; Kimura, S.; Kasuya, Y. Involvement of p38alpha mitogen-activated protein kinase in lung metastasis of tumor cells. *J Biol Chem* **2006,** 281, 36767-36775.

 doi:10.20944/preprints202310.0991.v1

38. Kim, C.; Cathey, A. L.; Watkins, D. J.; Mukherjee, B.; Rosario-Pabón, Z. Y.; Vélez-Vega, C. M.; Alshawabkeh, A. N.; Cordero, J. F.; Meeker, J. D. Maternal blood metal concentrations are associated with matrix metalloproteinases (MMPs) among pregnant women in Puerto Rico. *Environ Res* **2022,** 209, 112874.
39. Cosemans, J. Platelet-derived MMP-2 in the prevention of plaque formation: how many strokes is par? *Eur Heart J* **2022,** 43, 515-517.
40. Kang, D. S.; Lee, N.; Shin, D. Y.; Jang, Y. J.; Lee, S. H.; Lim, K. M.; Ahn, Y. S.; Lee, C. M.; Seo, Y. R. Network-based integrated analysis for toxic effects of high-concentration formaldehyde inhalation exposure through the toxicogenomic approach. *Sci Rep* **2022,** 12, 5645.
41. Wong, W. T.; Tian, X. Y.; Chen, Y.; Leung, F. P.; Liu, L.; Lee, H. K.; Ng, C. F.; Xu, A.; Yao, X.; Vanhoutte, P. M.; Tipoe, G. L.; Huang, Y. Bone morphogenic protein-4 impairs endothelial function through oxidative stress-dependent cyclooxygenase-2 upregulation: implications on hypertension. *Circ Res* **2010,** 107, 984-991.
42. Belenguer, G.; Duart-Abadia, P.; Jordán-Pla, A.; Domingo-Muelas, A.; Blasco-Chamarro, L.; Ferrón, S. R.; Morante-Redolat, J. M.; Fariñas, I. Adult neural stem cells are alerted by systemic inflammation through TNF-α receptor signaling. *Cell stem cell* **2021,** 28, 285-299.e9.
43. Tutone, M.; Virzi, A.; Almerico, A. M. Reverse screening on indicaxanthin from Opuntia ficus-indica as natural chemoactive and chemopreventive agent. *J Theor Biol* **2018,** 455, 147-160.